ADSORPTION OF NI(II) AND CO(II) IONS FROM AQUEOUS SOLUTION USING ACTIVATED CARBON BASED ON COFFEE AND COCOA SEED HUSK BIOMASS

MSc. Mónica Hernández Rodríguez[a,c] mhernandezr@ismm.edu.cu, Dr.C Jan Yperman[b] jan.yperman@uhasselt.be, Dr.C Robert Carleer[b] rcarleer@uhasselt.be, Dr.C José Falcón Hernández[d] falcon@uo.edu.c, Dr.C Alexis Otero Calvis[a] acalvis@ ismm.edu.cu

[a]*Mineral and Metallurgic Institute (ISMM), Moa, Holguín, Cuba,*

[b]*Research group of Applied and Analytical Chemistry, Hasselt University, Agoralaan building D, 3590-Diepenbeek, Belgium*

[c]*Faculty of Chemical Engineering, Universidad de Oriente, Santiago de Cuba, Cuba*

[d]*Department of Polymer and Carbonaceous Material, Faculty of Chemistry, Wroclaw University of Technology, Gdanska 7/9, 50-344 Wroclaw, Poland*

Abstract

The aim of this research is to relate surface chemistry and textural characteristics of activated carbon (AC) in the adsorption of Ni and Co ions present in single, bi and multi-elemental solutions, which simulates the wastewater from mineral processing in acid leaching technology. The chars were treated with Na_2S solution before activation process for pore development. Batch adsorption test were done as function of heavy metal concentration, adsorbent doses, temperature and adsorption time. The adsorption behavior was evaluated through isotherm models, thermodynamics and kinetics parameters. The adsorption of the metallic species is an endothermic and spontaneous nature, with the combination of physical and chemical forces. The kinetic behaviour is explain by a “surface enhancement” associated with highly energetic and heterogeneous surface. In multi-element solutions containing Ni(II), Co(II), Mn(II) and Mg(II) ions, the adsorption is enhanced for ACs pore development.

Keywords: Adsorption mechanism, coffee husk, cocoa seed husk

1. Introduction

Nowadays the increase of heavy metals in the environment is a major concern, for their toxicity and propensity to bio-accumulate in the food chain. They can cause harmful effects to the flora, fauna and humans even at low concentrations (Srivastava et al. 2011).

Standard levels of nickel and cobalt ions in drinking water are 0.2 mg/L and 0.05 mg/L, respectively. Mineral processing using acid leaching technology leaves about 40-45 mg/L of nickel (II) and 5 mg/L of cobalt (II) in the aquatic environment. The waste that contain these elements also has high quantities of manganese (II) and magnesium (II), making the recovery of nickel (II) and cobalt (II) a complex process. Therefore, development of effective methods for nickel (II) and cobalt (II) recovery from these industries effluents is a challenging situation.

The activated carbon (AC) is very effective in treating low metal-ion concentration in aqueous solutions (Youssef et al. 2004, Zang et al. 2005, Nadeem et al. 2006). The use of agricultural waste as activated carbon precursors is a renewable, less expensive and offers environmental advantages (Adib et al. 2015).

ACs application in adsorption process is mostly related with their surface chemistry and pore structure. Thus, the main purpose of researches in the last years is to obtain ACs with specific surface functionalities and/or to improve the micro and mesoporosity of adsorbents (Ariyadejwanich et al. 2003, Arami-Niya et al. 2011), through surface modification using techniques such as: acid or base treatment, impregnation with several chemical reagents and thermal process (Bhatnagar et al. 2013). Chemical treatment of AC prior activation produces more active sites into char structure, which afterward can develop to micro and mesopores during steam activation. The development of pores structure enhances AC adsorption capacity, where mesopores have a significantly role, acting as the main transport routes for the adsorbate to the micropores (Lyubchik et al. 2002, Carrier et al. 2012).

In this research, ACs are obtained by physical activation from coffee and cocoa seed husk. The chars were pre-treated with Na_2S solution for obtaining ACs with more pore structure development. Adsorption process of Ni and Co ions present in

single, bi and multi-elemental solutions is evaluated. Adsorption models (Langmuir, Freundlich and Dubinin–Radushkevich), thermodynamics, kinetics and characteristics of the adsorbent materials are also assessed.

2. Materials and methods

2.1. Chemicals and solutions for adsorption process

All reagents used were analytical grade and purchased from Merck. Stock solutions of 5000 mg/L for Ni(II), Co(II), Mn(II) and Mg(II) were prepared by dissolving $NiSO_4 \cdot 6H_2O$, $CoSO_4 \cdot 7H_2O$, $MnSO_4 \cdot H_2O$ or $MgSO_4 \cdot 7H_2O$ in Milli-Q water. All other solutions containing these metals ions were prepared by diluting the stock solutions. The pH of the solution was adjusted with 0.1 N NaOH or 0.1 N HCl solutions. The concentration of nickel ions was determined using an inductively coupled plasma spectrophotometer (Perkin Elmer Optima 3000 DV ICP-AES device with an axial plasma configuration).

2.2. Raw materials, preparation of activated carbons

Coffee husk and cocoa seed husk were acquired from the eastern region of Cuba. Activated carbon has been prepared from the above materials. Samples are first pyrolyzed in an oxygen-free atmosphere (N_2, 2 x 70 mL/min at 450 ° C) in a lab-scale reactor. The sample is continuously kept in motion by an Archimedes screw in order to achieve a uniform heat distribution. The reactor is heated up with a specially tailored heating mantle, and the temperature is checked using a thermocouple located inside the reactor. During the thermal treatment, the sample is subjected to a thermal cracking and volatilization. The biochar is activated in a second step.

The biochar is introduced in a horizontal quartz reactor and fixed with two quartz wool plugs. The biochar was heated up under a N_2 atmosphere to 850°C at 20°C/min. At 850°C the atmosphere was switched from nitrogen to water vapour (10 mL) to complete the activation process for 30 min and 39 min for coffee husk char and cocoa seed char, which were denoted as HAC and CAC respectively.

For the preparation pre-treated activated carbons 8 g of biochar was mixed with 50 mL of 0.1 N $Na_2S·9H_2O$ solution and dried overnight at 110°C for the complete evaporation of the solvent. Then, the impregnated biochar was conducted to activation process. After that was thoroughly washed with Milli-Q water and dried at 110°C for 24 h. The chemical pre-treated coffee husk and cocoa seed husk AC were coded as S-HAC and S-CAC respectively.

2.3. Characterization of adsorbent materials

Porous texture analysis has been carried out by N_2 and CO_2 adsorption at 77 and 273 K, respectively, in an Autosorb iQ apparatus (Quantachrome Instruments). The specific surface area (S_{BET}) was calculated from the N_2 sorption isotherm data using the BET (Brunauer, Emmett and Teller) method. The micropore volume ($V_{DR,N2}$) and the average micropore size ($L_{0,N2}$) were estimated by applying the Dubinin-Radushkevich and Stoeckli equations to data collected at low pressures ($p/p_0<0.015$) (Stoeckil et al. 1999). The Quenched-Solid Density Functional Theory (QSDFT) analysis (Neimark et al. 2009) was applied to the N_2 adsorption isotherms to determine pore size distribution (PSD).

The CO_2 isotherms at 273 K and low relative pressure $p/p_0<0.1$ are assumed to correspond to the adsorption taking place in the narrow micropores in the range of 0.4-0.8 nm (ultramicropores). These isotherm were used to calculate the ultramicropore volume ($V_{DR,CO2}$) and ultramicropore size ($L_{0,CO2}$) by means of the Dubinin-Radushkevich and Stoeckli equations, respectively (Stoeckil et al. 1999). The PSD was also calculated from the CO_2 isotherm data by applying the Non-Local Density Functional Theory (NLDFT) in order to characterize ultramicropores.

ATR measurements were performed to assess the functional groups involved in the adsorption mechanism. The dried samples were directly measured in the wavenumber range from 4000 to 600 cm^{-1} with a resolution of 4 cm^{-1} using a Bruker Vertex 70 equipped with a DTGS detector (32 scans) and diamond ATR crystal.

2.3. Effect of metal ion concentration

Adsorption test, for evaluating the initial concentration of Ni(II) and Co(II) were carried out at 25 ^{o}C in an Erlenmeyer of 250 mL. The amount of adsorbent (25 mg) was added to a 50 mL of Ni(II) or Co(II) solution with metal ion concentration between 30-180 mg/L and solution pH of 6. All experiments were performed during 24 h of contact time. After each experiment, the solution was filtered using a cellulose Ø 150 mm filtration paper and the final pH and concentration of metal ions was determined.

The amount of Ni(II) or Co(II) adsorbed q_e (mg/g) at equilibrium, was calculated using the following equation:

$$q_e = \frac{C_0 - C_e}{m} \times V \quad (1)$$

where c_0 and c_e are the initial and equilibrium concentration of metal ions respectively (mg/L). The real value of c_e was corrected taking into account the amount of Ni(II) or Co(II) that could have precipitated in the solutions because of the increase of final pH.

The removal percentage of adsorbed heavy metals was estimated by:

$$R_{emoval}(\%) = \frac{C_0 - C_e}{C_0} \times 100 \quad (2)$$

2.4. Adsorption isotherms

Freundlich isotherm is an empirical model and can be applied to multilayer adsorption, with non-uniform distribution of adsorption, heat and affinities over the heterogeneous surface (Olivera et al. 2008) and in linear form it is given by:

$$\log q_e = \log K_F + \frac{1}{n} \log C_e \quad (3)$$

where K_F is related with the adsorption capacity and n is related to the heterogeneity and the adsorption intensity.

Langmuir isotherm is based on a theoretical model and assumes monolayer adsorption over an energetically homogeneous adsorbent surface containing a finite number of adsorption sites. It does not take into account interactions between adsorbed molecules (Kundo et al. 2006, Pérez et al. 2007). It can be represented by the following linear equation:

$$\frac{1}{q_e} = \frac{1}{q_m} + \left(\frac{1}{K_L q_m}\right)\frac{1}{C_e}$$

(4)

where q_m and K_L are constants related to the maximum adsorption capacity (mg/g) and the adsorption energy (L/mg), respectively. Hereby, a dimensionless constant, known as separation factor (R_L) can be defined by:

$$R_L = \frac{1}{1+K_L C_0}$$

(5)

R_L value indicates the adsorption nature to be either unfavourable (R_L >1), linear (R_L =1), favourable (0 <R_L <1) or irreversible (R_L =0).

The Dubinin–Radushkevich (D–R) is an empirical model initially conceived for the adsorption of subcritical vapours onto micropore solids following a pore filling mechanism. The approach was usually applied to distinguish the physical and chemical adsorption of metal ions (Dubinin 1960). The linear model is given by:

$$\ln q_e = \ln q_s - K_D \varepsilon^2$$

(6)

$$\varepsilon = RT\ ln\left(1 + \frac{1}{C_e}\right)$$

(7)

where q_s is the maximum sorption capacity of the adsorbent (mg/g), ε is the Polanyi sorption potential and K_D (mol^2/J^2) is a constant related to the mean energy of sorption per mole of adsorbate as it is transferred from the bulk solution to the surface of the solid. This energy *E* is determined by the following equation:

$$E = \frac{1}{\sqrt{2\,K_D}}$$

(8)

The parameter *E* is used for estimating the type of adsorption. If this value is below 8 kJ/mol the adsorption type can be explained by physical adsorption, between 8 and 16 kJ/mol the adsorption type can be explained by ion exchange, and over 16 kJ/mol the adsorption type can be explained by a stronger chemical adsorption.

2.5. Temperature effect

The effect of temperature in the adsorption process was evaluated among 25–45 ^{o}C in an Erlenmeyer of 250 mL. The adsorbent (25 mg) was added to a 50 mL of Ni(II) or Co(II) solution with metal ion concentration between 30-180 mg/L and solution pH of 6. The Erlenmeyers were sealed and shaken during 24 h. After agitation, the adsorbent was removed by filtration and 10 mL of solution was taken to determine the concentration of metal ions.

2.6. Thermodynamics and kinetics parameters

The free energy change ($\Delta G°$), enthalpy change ($\Delta H°$), and entropy change ($\Delta S°$) of Ni and Co ions were determined, to know the internal energy changes associated with adsorption process. The values of $\Delta H°$, $\Delta S°$ and $\Delta G°$ can be obtained from (Ahmad et al. 2011):

$$\ln K_e = \frac{\Delta S°}{R} - \frac{\Delta H°}{RT}$$

(9)

$$\Delta G° = -RT\,lnK_e$$

(10)

where K_e is the equilibrium constant. The values of $\Delta H°$ (kJ/mol) and $\Delta S°$ (J/molK) can be calculated, respectively from the slope and intercept of lnK_e versus 1/T plot.

According to Liu 2009, for an adsorption process described as follows:

A+B↔AB

(11)

where A is the free adsorptive solute molecules, B is the vacant sites on the adsorbent, and AB the occupied sites. The equilibrium constant K_e is defined as K_a and this one is equal to Langmuir constant (K_L) in L/mol, K_a=K_L(1 molL^{-1}) for a diluted solution of adsorbate. K_a is defined as:

$$K_a = \frac{(activity\ of\ occupied\ sites)}{(activity\ of\ vacant\ sites)(activity\ of\ solute\ in\ solution)} = \frac{(AB)}{(B)\cdot(A)}$$

(12)

Considering that the activity coefficients of the occupied and vacant sites are the same, the Eq. 12 becomes:

$$K_a = \frac{\theta_e}{(1-\theta_e)\gamma_e C_e}$$

(13)

were θ_e is the fraction of the surface covered at equilibrium, θ_e = q_e/q_m and γ_e is the activity coefficient of the adsorbate in the solution at equilibrium. Considering a dilute solution ($\gamma_e = 1$) the equilibrium constant could be rewrite as:

$$K_a = \frac{q_e/q_m}{\left(1-q_e/q_m\right)C_e}$$

(14)

For the charged adsorbate as Ni or Co ions, the effect of ionic strength was neglected and subsequently the thermodynamic parameters were calculated as an approximation.

The characteristics of kinetics process allow understanding the adsorption mechanism. The pseudo first-order rate equation of Lagergren is a simply and usually kinetic model used in the evaluation of adsorption of solute from a liquid solution (Kshama et al. 2011). Pseudo-second order kinetic model is based on the assumption that the rate-limiting step is chemisorption in nature and mechanism could involve valence forces by sharing or through the exchange of electrons between adsorbent and adsorbate (Srivastava et al. 2011). Linearized models can be expressed for the following equations:

$$log(q_e - q_t) = \log q_e - \frac{k_1}{2.303} t$$

(15)

$$\frac{t}{q_t} = \frac{1}{k_2 q_e^2} + \frac{1}{q_e} t$$

(16)

Where k_1 and k_2 are the adsorption rate constants of first and second order kinetic models, in min^{-1} and g/(mg min), respectively; q_e and q_t, in mg/g, are equilibrium adsorption capacity at equilibrium time and at time t. From the slope and the intercept of each linear plot, the adsorption rate constants (k_1 and k_2) can be calculated.

2.7. Activation Energy

Arrhenius equation allows to determinate the activation energy (E_a) throughout the linearized equation (Aksu 2002):

$$\ln k = \ln A - \frac{E_a}{RT}$$

(17)

Where k the rate constant value for the metal adsorption, A is the frequency factor related with the possibility that the collisions are favourably oriented for reaction, E_a is the activation energy in kJ/mol, T the absolute temperature (K) and R the universal gas constant (8.314 J/mol K). The value of E_a can be estimated by the slope of graph ln k vs 1000/T.

2.8. Adsorption test in multi-element solution

A multi-element solution containing Ni(II), Co(II), Mg(II) and Mn(II) ions was prepared. The concentration of the metal ions was similar to the generated wastewater in mineral processing of acid leaching technology. The adsorption test in batch mode was done at the best temperature in sealed Erlenmeyers of 250 mL containing 50 mL of multi-element solution, pH 6 and adsorbent doses of 62.5 and 125 mg (1.25 and 2.5 g/L) during 24 h of contact time at 50 rpm of shake speed.

3. Results and discussion

3.1. Characterization of adsorbent materials

The ATR-FTIR spectra (Fig. 1) reveals more intense absorption peaks for CAC. For HAC the bands located at 3639 cm^{-1}correspond with no bonded hydroxy group –OH stretch; 2175 cm^{-1} are related with acetylenic groups confirmed for C–H bending vibration around 630 cm^{-1}; 1373 cm^{-1} is characteristic of phenol or tertiary alcohol –OH stretch; the several peaks between 850-610 cm^{-1} can be attributed to aromatic C–H and alcohol –OH out of plane bend. After chemical pre-treatment process, the band corresponding to acetylenic groups disappears, for the saturation of C≡C bond, and the vibration of aromatic C–H out of plane bend is less intense. The appearance of bands at 1251 cm^{-1} and 998 cm^{-1} suggest the conversion of some alcohol to aromatic ethers and carboxylic anhydric groups. CAC has peaks at 3188 cm^{-1} (hydroxy group –OH stretch), 2362 cm^{-1} (acetylenic groups), 1511 cm^{-1}(aromatic C=C–C vibration stretch), 1385 cm^{-1} (methyl $–CH_3$ group), 1038 cm^{-1} (primary alcohol C–O stretch or C–C skeletal vibration), and several peaks among 900-620 cm^{-1} (aromatic C–H and alcohol –OH out of plane bend). Chemical pre-treatment of CAC conducts to the removal of almost all functional groups, just the band corresponded to primary alcohol C–O stretch or C–C skeletal vibration is observed.

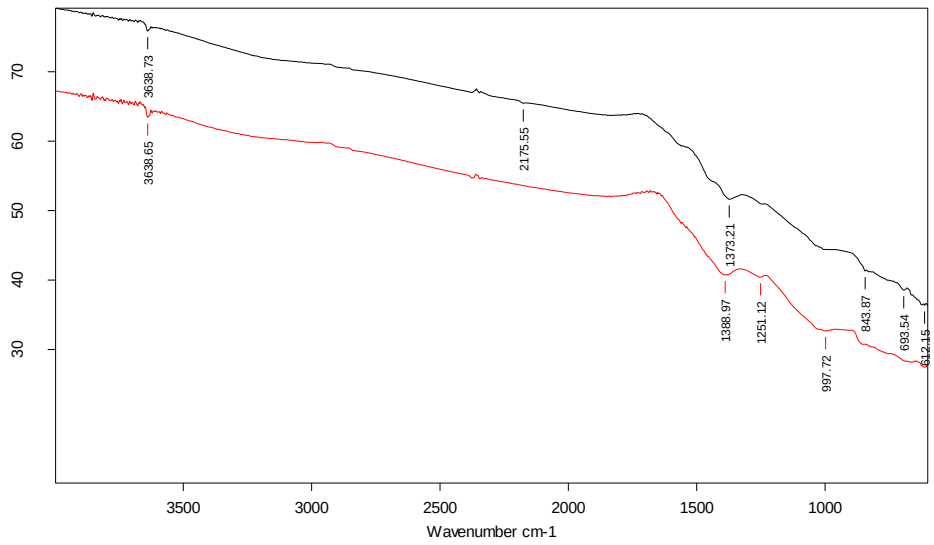

(a)

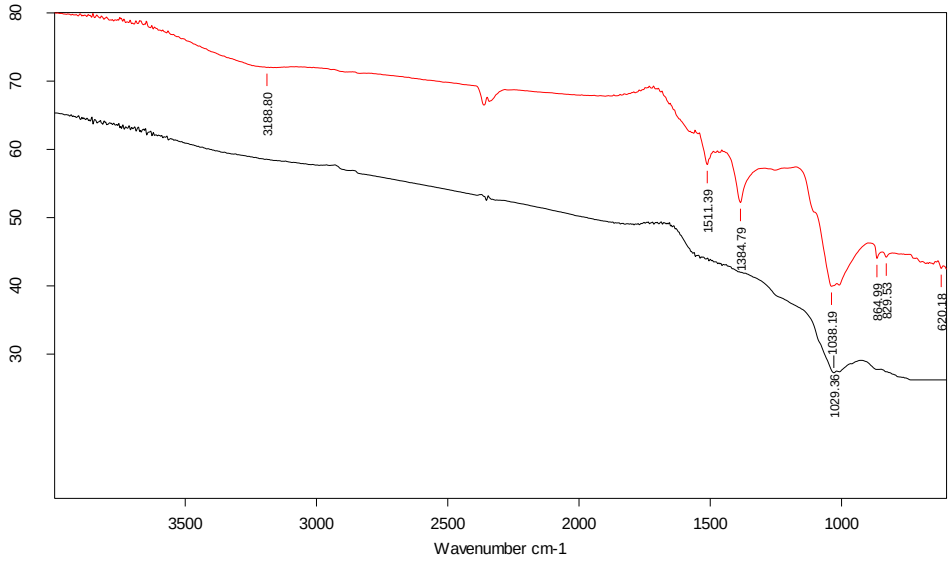

(b)

Fig. 1 ATR spectra (a) ── HAC, ──S-HAC, (b) ── CAC, ── S-CAC.

Fig. 2 depicts the nitrogen adsorption-desorption isotherms at 77 K for the samples. For CAC the isotherm shape shows a sharply increase at low relative pressure of p/p_0 and reach a plateau in a broad range of p/p_0. This shape could be classified as Type I isotherm, characteristics of microporous materials, having mainly narrow micropores (Thommes et al. 2015). However, for HAC, S-HAC and S-CAC the isotherm shape continually increases until the end of relative pressure. These samples have a combination of Type I with Type IV isotherms, characteristic of microporous and mesoporous materials (Thommes et al. 2015). Chemical treatment of the chars conducts to obtain greater nitrogen uptakes at the same value of relative pressure (p/p_0) and more intense hysteretic loops during desorption, usually associated with capillary condensation in mesopores (Thommes et al. 2015). The development of mesoporosity (less relation V_{DR}/V_T), micropore volume (V_{DR}), superficial area (S_{BET}) and total pore volume (V_T) (Table 1) of S-HAC and S-CAC prove that pre-treatment of chars with Na_2S produce more active sites, which consequently developed into micro and mesopores during steam activation (Ariyadejwanich et al. 2003). The pore size distribution determined by QSDFT method confirmed that S-HAC and S-CAC exhibit more

intense maximum at a pore width of 0.57 nm, than HAC and CAC (Fig. 2b). Others maximum center are found at 0.79, 1.01, 1.54 nm for CAC; 0.85, 1.54 nm for HAC; 1.01, 1.54 nm for S-CAC and S-HAC respectively.

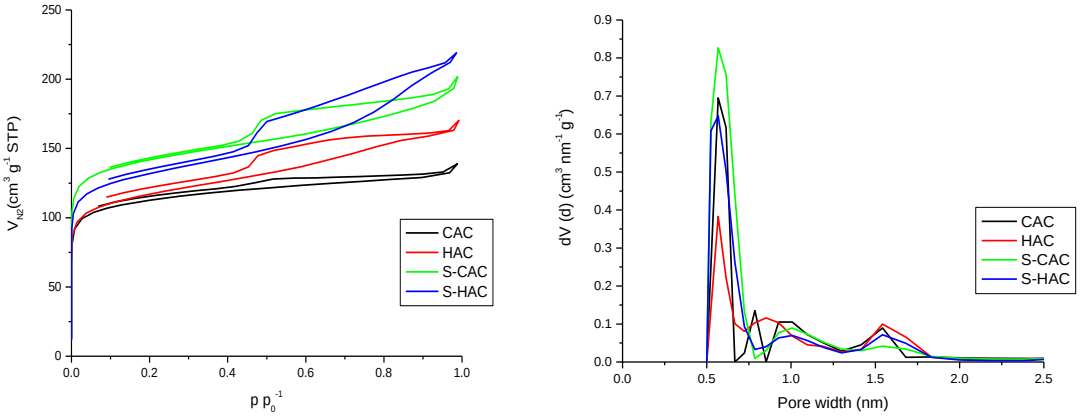

(a) (b)

Fig. 2 Nitrogen adsorption-desorption isotherms at 77 K (a) and QSDFT pore size distribution (b).

Table 1 Textural parameters for HAC, S-HAC, CAC and S-CAC

Sample	S_{BET}	V_T*	V_{DR}	V_{DR}/V_T	L_0**	$V_{DR,CO2}$	$S_{0,CO2}$***	$L_{0,CO2}$**
	m^2/g	cm^3/g	cm^3/g		nm	cm^3/g	m^2/g	nm
HAC	438	0.250	0.168	0.67	0.84	0.166	976	0.34
S-HAC	494	0.326	0.189	0.58	0.77	0.172	860	0.40
CAC	428	0.204	0.165	0.81	0.81	0.140	778	0.36
S-CAC	537	0.294	0.205	0.69	0.74	0.160	800	0.40

* at p/p_0~0.96 for pores smaller than 50 nm
** $L_0=10.8/(E_0-11.4)$
***$S_{0,CO2}=(2000\cdot V_{DR,CO2})/L_{0,CO2}$

The prepared ACs were analyzed by sorption of CO_2 to characterize ultramicropores. Fig. 3 shows the CO_2 adsorption isotherms (a) and the pore size

distribution determined by NLDFT method (b) in the range of ultramicropores. The ACs show a bimodal distribution of ultramicropores size with maximum centers at 0.35 nm and between 0.52-0.55 nm for all samples. The volume and average width of ultramicropores are greater for S-HAC and S-CAC compared with HAC and CAC.

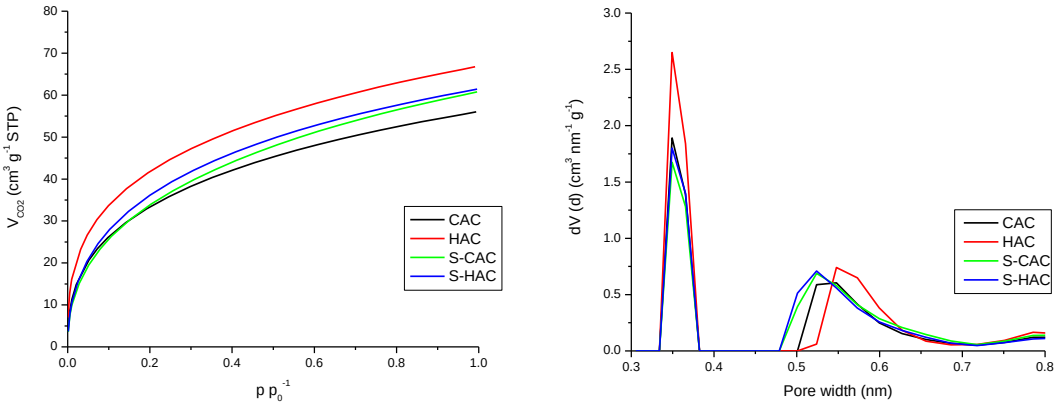

(a) (b)

Fig. 3 CO_2 adsorption isotherms at 273 K (a) and NLDFT pore size distribution (b).

3.2. Adsorption isotherms modeling

Adsorption isotherms modeling is an important step to assess adsorption behaviour. At 25 ºC, HAC and CAC are better described for Langmuir and D-R models (Table 2). However, S-HAC and S-CAC show a better fit with Langmuir followed by Freundlich model. Beside the best fit of Langmuir model, adsorption system presents a certain degree of heterogeneity due to the existence of surface functionalities (Fig. 1) with different affinities to the adsorbates. In all cases, the separation factor (R_L) is between 0-1, demonstrating a favourable adsorption process. The maximum adsorption capacities (q_m) are bigger for CAC and HAC, the ACs with less surface area (Table 1) but higher surface functionalities (Fig. 1). The mean energy of sorption per mole of adsorbate (*E*) is less than 8 kJ/mol,

corresponding rather with a physical adsorption process. These results indicate that at low temperature, adsorption process of ACs from coffee and cocoa seed husk is related more with surface functionalities than pore structure development or surface area.

Table 2 Isotherm parameters for Ni and Co ions

Carbon	Ni						Co					
	Langmuir		Freundlich		D-R		Langmuir		Freundlich		D-R	
HAC	R^2	0.96	R^2	0.77	R^2	0.99	R^2	0.97	R^2	0.84	R^2	0.97
	q_m	92.4	K_F	46.8	q_s	87.2	q_m	101.7	K_F	34.7	q_s	92.1
	K_L	0.25	n	6.37	K_D	3E-06	K_L	0.14	n	4.44	K_D	6E-06
	R_L	0.02-0.10			E	0.40	R_L	0.03-0.18			E	0.28
CAC	R^2	0.98	R^2	0.83	R^2	0.98	R^2	0.945	R^2	0.78	R^2	0.99
	q_m	105.8	K_F	47.3	q_s	86.1	q_m	107.5	K_F	33.0	q_s	97.0
	K_L	0.27	n	5.71	K_D	2E-06	K_L	0.12	n	4.05	K_D	7E-06
	R_L	0.02-0.10			E	0.50	R_L	0.04-0.20			E	0.26
S-HAC	R^2	0.94	R^2	0.93	R^2	0.86	R^2	0.97	R^2	0.93	R^2	0.92
	q_m	57.0	K_F	18.4	q_s	50.3	q_m	51.7	K_F	11.8	q_s	43.7
	K_L	0.08	n	4.54	K_D	2E-05	K_L	0.05	n	3.55	K_D	3E-05
	R_L	0.06-0.27			E	0.15	R_L	0.09-0.38			E	0.12
S-CAC	R^2	0.99	R^2	0.95	R^2	0.93	R^2	0.96	R^2	0.94	R^2	0.87
	q_m	40.0	K_F	10.3	q_s	34.3	q_m	46.0	K_F	16.5	q_s	41.3
	K_L	0.05	n	3.90	K_D	3E-05	K_L	0.09	n	5.06	K_D	2E-05
	R_L	0.08-0.36			E	0.12	R_L	0.05-0.26			E	0.15

3.3. Temperature effect

The effect of temperature is depicted in Fig. 4-5. The increment of temperature tends to improve the adsorption of target ions in the active places; this change is more abrupt for Na_2S pre-treated ACs. S-HAC and S-CAC reached at 45 ^oC adsorption capacities greater than HAC and CAC respectively. With the increment of temperature, the role of surface functionalities is less important and the ACs with more pore development achieved better results.

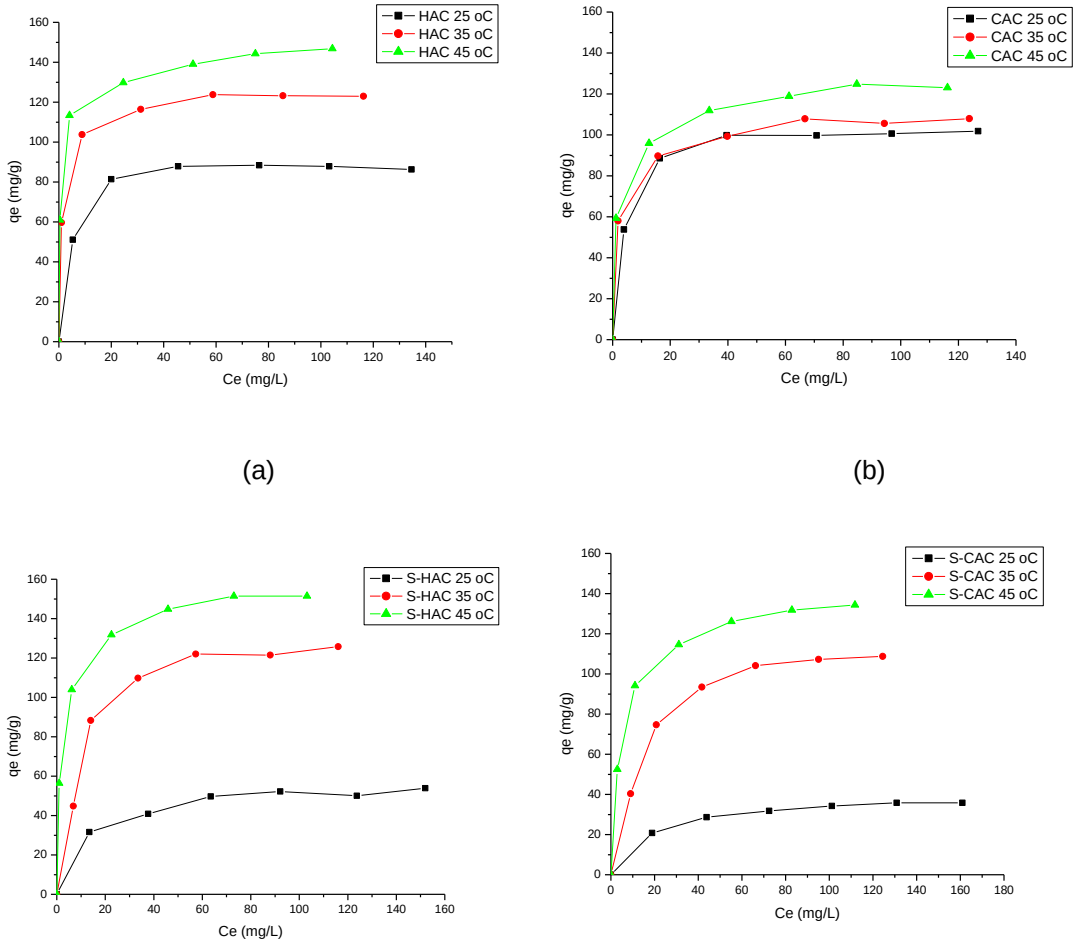

Fig. 4 Effect of temperature for Ni ions (a) HAC, (b) CAC, (c) S-HAC, (d) S-CAC (m= 25 mg, C_0 = 30-180 mg/L, V = 50 mL, pH = 6, shake speed 50 rpm, t = 24 h).

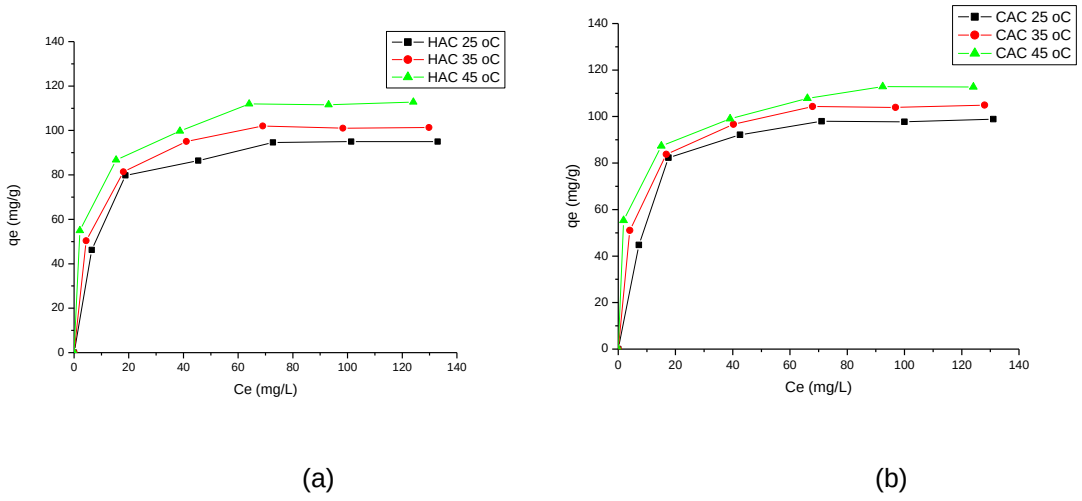

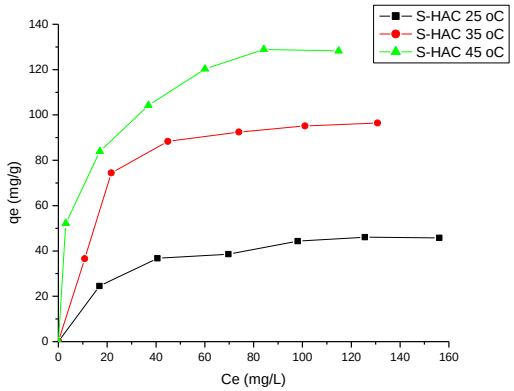

(c)

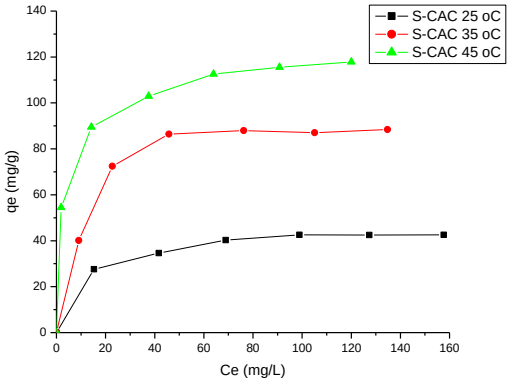

(d)

Fig. 5 Effect of temperature for Co ions (a) HAC, (b) CAC, (c) S-HAC, (d) S-CAC (m= 25 mg, C_0 = 30-180 mg/L, V = 50 mL, pH = 6, shake speed 50 rpm, t = 24 h).

3.4. Thermodynamic and kinetic parameters

Table 3 evidences the approximate thermodynamic parameters (according eqs. 4) involve in the adsorption of Ni and Co ions when the temperature was increased from 25 ºC (298 K) until 45 ºC (318 K). As ΔH^{o} is positive and ΔG^{o} is negative, the adsorption of the metallic species has an endothermic and spontaneous nature. The adsorption process is favoured at higher temperatures. The value of ΔH^{o} are between 23-75 kJ/mol, suggesting more to a chemical bonding process beside the value of mean energy (*E* less than 8 kJ/mol) from D-R isotherm model. These results propose the combination of physical and chemical forces during the adsorption for all ACs.

Table 3 Thermodynamic parameters for ACs

	Ni					Co				
	ΔH^{o}	ΔS^{o}	ΔG^{o} kJ/mol			ΔH^{o}	ΔS^{o}	ΔG^{o} kJ/mol		
	kJ/mol	J/molK	298K	308K	318K	kJ/mol	J/molK	298K	308K	318K
	Based K_L (Eq. 4)									
HAC	74.7	331.4	-23.8	-27.7	-30.4	38.8	205.2	-22.4	-23.9	-26.5
CAC	37.0	205.6	-24.0	-26.7	-28.1	50.4	243.0	-22.1	-24.1	-26.9
S-HAC	65.1	287.5	-21.1	-22.0	-26.9	39.3	198.2	-19.9	-21.2	-23.9
S-CAC	47.6	225.9	-20.1	-21.0	-24.6	57.7	263.1	-21.2	-22.1	-26.6

The kinetics was also done for Ni ions in single and bi-elemental solutions (Ni+Co ions) according with their concentration in the wastewater for acid leaching process. Fig. 6 shows that the increment of temperature favours the kinetics of Ni ions. The equilibrium is reached very faster for HAC and S-HAC (around 2 h of contact time), while for CAC and S-CAC at 25 ^{o}C takes 3 and 5 h. At higher temperatures (35 and 45 ^{o}C) the equilibrium time decrease until 2 h for CAC and S-CAC respectively. Kinetics of Co ions (Figures not shown) at low concentration (5 mg/L) occurs also very rapidly achieving equilibrium times around 1 h at 35 and 45 ^{o}C for all adsorbent materials.

The differences in kinetics behaviour seems to be related with surface functionalities, as the increment of qt_{Ni} is more sharply for HAC and CAC at any temperature than S-HAC and S-CAC. In addition, the mesopores play an important role providing the degree of accessibility to the micropores, in this case the ACs with more mesoporosity (HAC and S-HAC) adsorb faster than CAC and S-CAC. With the increment of temperature, the difference in Ni uptake is less remarkable because higher temperatures facilitate the diffusion of the adsorbate into the pores of the adsorbent materials.

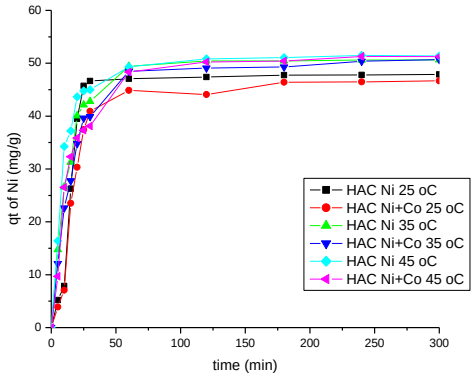

(a)

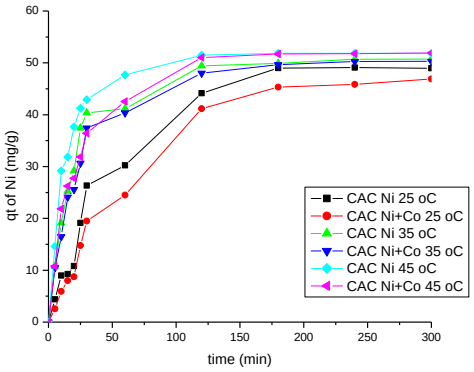

(b)

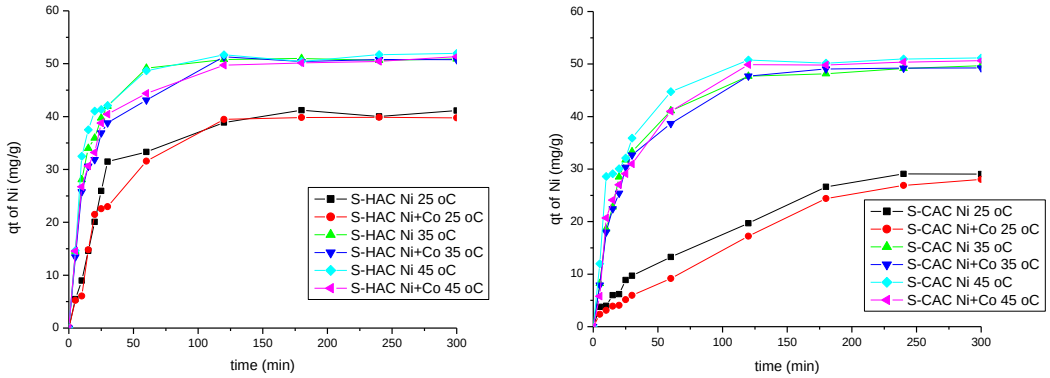

(c) (d)

Fig. 6 Adsorption kinetics of Ni from Ni and Ni+Co solution (a) HAC, (b) CAC, (c) S-HAC, (d) S-CAC (m=37.5 mg, C_0 Ni= 40 mg/L, C_0 Co= 5 mg/L V = 50 mL, pH = 6, shake speed 50 rpm).

Kinetics parameters for Ni ions in single and bi-elemental solutions (Ni+Co ions) were obtained fitting kinetic data to pseudo-first and pseudo-second order (Table 4). HAC and S-HAC show a good agreement with pseudo second-order model in the all range of temperature studied, however CAC and S-CAC can be described for pseudo-first and pseudo-second order models, but with the increment of temperature pseudo-first order model is less representative of kinetic behaviour. The best fit of pseudo-second order model suggest that the rate-limiting step could be chemisorption promoted either by covalent forces, through sharing or exchanging electrons, and this mechanism of adsorption is improved with the increment of temperature.

Table 4 Kinetic parameters for ACs at different temperatures

Carbon	Ni (single solution) Pseudo-first order		Ni (single solution) Pseudo-second order		Ni (bi-elemental solution) Pseudo-first order		Ni (bi-elemental solution) Pseudo-second order	
At 25 ºC								
HAC	R^2	0.63	R^2	0.97	R^2	0.81	R^2	0.96
	k_1	0.014	k_2	0.001	k_1	0.014	k_2	0.0007
CAC	R^2	0.91	R^2	0.97	R^2	0.98	R^2	0.96
	k_1	0.023	k_2	0.0003	k_1	0.0152	k_2	0.0002
S-HAC	R^2	0.82	R^2	0.99	R^2	0.86	R^2	0.98
	k_1	0.0175	k_2	0.0008	k_1	0.0244	k_2	0.0007
S-CAC	R^2	0.96	R^2	0.96	R^2	0.78	R^2	0.76
	k_1	0.014	k_2	0.0003	k_1	0.0173	k_2	7.2E-05
At 35 ºC								

	R^2	0.76	R^2	0.99	R^2	0.90	R^2	0.99
HAC	k_1	0.0134	k_2	0.0025	k_1	0.0157	k_2	0.0017
	R^2	0.95	R^2	0.99	R^2	0.94	R^2	0.99
CAC	k_1	0.0177	k_2	0.0012	k_1	0.015	k_2	0.001
	R^2	0.77	R^2	0.99	R^2	0.68	R^2	0.99
S-HAC	k_1	0.0147	k_2	0.0023	k_1	0.0145	k_2	0.0016
	R^2	0.97	R^2	0.99	R^2	0.92	R^2	0.99
S-CAC	k_1	0.0168	k_2	0.001	k_1	0.0159	k_2	0.0009
At 45 ºC								
	R^2	0.80	R^2	0.99	R^2	0.85	R^2	0.99
HAC	k_1	0.0117	k_2	0.0033	k_1	0.0127	k_2	0.0016
	R^2	0.87	R^2	0.99	R^2	0.93	R^2	0.99
CAC	k_1	0.0175	k_2	0.0021	k_1	0.0193	k_2	0.001
	R^2	0.87	R^2	0.99	R^2	0.92	R^2	0.99
S-HAC	k_1	0.0184	k_2	0.0025	k_1	0.0124	k_2	0.0017
	R^2	0.87	R^2	0.99	R^2	0.93	R^2	0.99
S-CAC	k_1	0.0136	k_2	0.0014	k_1	0.0175	k_2	0.0008

3.6. Activation energy results

Activation energy (E_a) and frequency factor (A) for Ni ions obtained from fitting ln k_2 (as better agree of pseudo-second order model) vs 1000/T is exposed in Table 5. Values of activation energy for Ni ions greater than 30 kJ/mol confirm that the rate controlling step is kinetic sorption (Ho et al. 2000), which is strongly dependent of temperature. The kinetic behaviour is explain by a “surface enhancement”, associated with highly energetic and heterogeneous surface (Ho et al. 2000).

Table 5 Parameters from Arrhenius equation

	Arrhenius equation parameters		
Carbon	E_a (kJ/mol)	A	R^2
HAC	48.33	3.22E+05	0.9285
CAC	84.73	2.06E+11	0.9409
S-HAC	43.59	4.26E+04	0.8238
S-CAC	57.85	4.96E+06	0.9184

3.7. Adsorption of Ni and Co ions in multi-element solution

Adsorption test in multi-element solution was done simulating the concentration of metal ions in the wastewater from acid leaching process: 40 mg/L of Ni(II), 5 mg/L of Co(II), 1062 mg/L of Mg(II) and 1858 mg/L of Mn(II). The experiments were carried out at 45 ^{o}C at different adsorbent doses shown in Table 6. The affinity of ACs for metal ions taking into account the removal % follows the order: Ni(II)>Co(II)>Mn(II)>Mg(II).

At adsorbent doses of 1.25 g/L Na_2S pre-treatment process of coffee husk AC (S-HAC) allows to improve the removal of Ni(II) in 12.84% and Co(II) in 4.39% in comparison with the removals achieved for HAC. Meanwhile for Mn(II) and Mg(II) the removals is kept almost constant. For cocoa seed husk AC, chemical pre-treatment (S-CAC) increase the removals of Mn(II) and Mg(II), keeping the amount of Ni(II) and Co(II) adsorbed practically constant.

At adsorbent doses of 2.50 g/L the final solution pH increase at values > 9.0 when is used HAC and CAC, causing a precipitation of heavy metal ions and diminishing the real value of qe and removal (%). The removals and adsorption capacities shown in Table 6 under this condition where adjusted taking into account the amount of metal ions precipitated. S-HAC have removals of Ni(II) and Co(II) of 69.27 and 48.68 %, exceeding in 30.44 and 21.19 % the achieved with S-CAC. S-HAC seem to be more profitable for the adsorption of Ni(II) and Co(II), meanwhile S-CAC for the recovery of Mn(II) and Mg(II).

These results suggest that in spite of adsorption process is explain for a “surface enhancement”, were functional groups have an essential role, in multi-elemental solutions the development of ACs pore structures due to Na_2S pre-treatment can provide more available adsorption surface than ACs without chemical pre-treatment. Also S-HAC and S-CAC allow the recovery of Ni(II) and Co(II) ions at bigger adsorbent doses without heavy metal precipitation, which in view of industrial application is also interesting.

Table 6 Adsorption results in multi-element solution

	Adsorbent	Final	Ni		Co		Mn		Mg	
Carbon	doses (g/L)	pH	qe (mg/g)	R %	qe (mg/g)	R %	qe (mg/g)	R %	qe (mg/g)	R %

HAC		7.38	6.23	39.14	0.68	33.91	122.08	16.43	24.68	5.81
CAC	1.25	7.33	3.97	24.97	0.27	13.61	32.68	4.40	10.24	2.41
S-HAC		7.08	8.27	51.98	0.77	38.30	120.60	16.23	27.28	6.42
S-CAC		7.15	3.78	23.76	0.33	16.46	119.92	16.14	25.88	6.09
HAC		9.03	4.10	51.59	0.38	37.22	80.68	21.71	11.68	5.50
CAC	2.50	9.22	3.01	37.89	0.25	25.13	47.90	12.86	8.62	4.06
S-HAC		7.22	5.51	69.27	0.49	48.68	104.10	28.01	14.34	6.75
S-CAC		7.31	3.09	38.83	0.28	27.49	82.46	22.19	13.12	6.18

4. Conclusions

The role of surface chemistry and textural characteristics of ACs from coffee and cocoa seed husk in the adsorption of Ni and Co ions was successfully studied. Chemical pre-treatment of ACs with Na_2S conducts to create more active sites into chars, which consequently developed into micro and mesopores during steam activation, also the treatment decrease the functional groups present in carbon surface. The adsorption of the metallic species is an endothermic and spontaneous nature, with the combination of physical and chemical forces. The rate-controlling step is kinetic sorption and their behaviour is explaining by a “surface enhancement”. In multi-element solutions containing Ni(II), Co(II), Mn(II) and Mg(II) ions, the adsorption is enhanced for ACs pore development. Na_2S chemical pre-treatment of ACs seem to be more interesting for the industrial applications.

References

Adib Yahya M., Al-Qodah Z., Zanariah Ngah C.W., Agricultural bio-waste materials as potential sustainable precursors used for activated carbon production: A review. Renewable and Sustainable Energy Reviews 46 (2015) 218–235.

Ahmad M.A., Rahman N.K., Equilibrium, kinetics and thermodynamic of Remazol Brilliant Orange 3R dye adsorption on coffee husk-based activated carbon, Chem. Eng. J. 170 (2011) 154–161.

Aksu Z., Determination of the equilibrium, kinetic and thermodynamic parameters of the batch adsorption of Ni(II) ions on to Chlorella vulgaris. Process Biochem. 38 (2002) 89–99.

Arami-Niya A., Ashri Wan Daud W. M., Mjalli F. S., Comparative study of the textural characteristics of oil palm shell activated carbon produced by chemical and physical activation for methane adsorption. Chemical Engineering Research and Design 89 (2011) 657–664.

Ariyadejwanich P., Tanthapanichakoon W., Nakagawa K., Mukai S.R., Tamon H., Preparation and characterization of mesoporous activated carbon from waste tires. Carbon 41 (2003) 157–164.

Bhatnagar A., Hogland W., Marques M., Sillanpää M., An overview of the modification methods of activated carbon for its water treatment applications. Chemical Engineering Journal 219 (2013) 499–511.

Carrier M., Neomagus H. W., Görgens J., Knoetze J. H., Influence of Chemical Pretreatment on the Internal Structure and Reactivity of Pyrolysis Chars Produced from Sugar Cane Bagasse. Energy Fuels 26 (2012) 4497−4506.

Dubinin M.M., The potential theory of adsorption of gases and vapors for adsorbents with energetically non-uniform surface, Chem. Rev. 60 (1960) 235–266.

Ho Y.S., Ng J.C.Y., McKay G., Kinetics of pollutant sorption by biosorbents: Review. Separation and purification methods 29 (2) 189–232 (2000).

Kshama A., Shroff K., Varsha V., Kinetics and equilibrium studies on biosorption of nickel from aqueous solution by dead fungal biomass of Mucor hiemalis. Chemical Engineering Journal 171 (2011) 1234–1245.

Kundu S., Gupta A.K., Arsenic adsorption onto iron oxide-coated cement (IOCC): regression analysis of equilibrium data with several isotherm models and their optimization, Chem. Eng. J. 122 (2006) 93–106.

Liu Y., Is the Free Energy Change of Adsorption Correctly Calculated? J. Chem. Eng. Data 54 (2009) 1981–1985.

Lyubchik S.B., Benoit R., Beguin F., Influence of chemical modification of anthracite on the porosity of the resulting activated carbons. Carbon 40 (2002) 1287–1294.

Nadeem M., Mahmood A., Shahid S.A., Shah S.S., Khalid A.M., McKay G., Sorption of lead from aqueous solution by chemically modified carbon adsorbents. J. Hazard. Mater. 138 (2006) 604–613.

Neimark A.V., Lin Y., Ravikovitch P.I., Thommes M., Quenched solid density functional theory and pore size analysis of micro-mesoporous carbons, Carbon 47 (2009) 1617-1628.

Oliveira W.E., Franca A. S., Oliveira L.S., Rocha S.D., Untreated coffee husks as biosorbents for the removal of heavy metals from aqueous solutions, J. Hazard. Mater. 152 (2008) 1073–1081.

Pérez Marín A.B., Meseguer Zapata V., Ortuno J.F., Aguilar M., Sáez J., Llorens M., Removal of cadmium from aqueous solutions by adsorption onto orange waste, J. Hazard. Mater. B 139 (2007) 122–131.

Srivastava V., Weng C. H., Singh V. K., Sharma Y. C., Adsorption of Nickel Ions from Aqueous Solutions by Nano Alumina: Kinetic, Mass Transfer, and Equilibrium Studies. J. Chem. Eng. Data 56 (2011) 1414–1422.

Stoeckil F., Daguerre E., Guillot A., The development of micropore volumes and widths during physical activation of various precursors, Carbon 37 (1999) 2075-2077.

Stoeckli F., Lopez M.V., Moreno Castilla C., Adsorption of phenolic compounds from aqueous solutions, by activated carbons, described by the Dubinin−Astakhov equation, Langmuir 17 (2001) 3301-3306.

Thommes M., Kaneko K., Neimark A. V., Olivier J. P., Rodriguez Reinoso F., Rouquerol J., Sing K. S.W., Physisorption of gases, with special reference to the evaluation of surface area and pore size distribution (IUPAC Technical Report). Pure Appl. Chem. (2015).

Youssef A.M., El-Nabarawy T., Samra S.E., Sorption properties of chemically-activated carbons: 1. Sorption of cadmium (II) ions. Colloids Surf. A Physicochem. Eng. Asp. 235 (2004) 153–163.

Zhang F-S., Nriagu J.O., Itoh H., Mercury removal from water using activated carbons derived from organic sewage sludge. Water Res. 39 (2005) 389–395.